Nuclear Engineering and Design 320 (2017) 269–281

Contents lists available at ScienceDirect

Nuclear Engineering and Design

journal homepage: www.elsevier.com/locate/nucengdes

In-containment source term predictability of ASTEC-Na: Major insights from data-predictions benchmarking

L.E. Herranz [a,*], M. Garcia [a], L. Lebel [b], F. Mascari [c], C. Spengler [d]

[a] CIEMAT, Unit of Nuclear Safety Research, Av. Complutense, 40, 28040 Madrid, Spain
[b] Institut de Radioprotection et de Sûreté Nucléaire (IRSN), Nuclear Safety Division, Saint-Paul-lez-Durance, France
[c] Italian National Agency for New Technologies, Energy and Sustainable Economic Development (ENEA), Bologna, Italy
[d] Gesellschaft für Anlagen-und Reaktorsicherheit (GRS), gGmbH, Cologne, Germany

HIGHLIGHTS

- In-containment Na aerosol data retrieved and gathered for code validation.
- Comparison of ASTEC-Na models for Na pool fires and aerosol ageing to data.
- Generic trends captured through a heavy models parametrization.
- Need for qualified data from representative experiments during Na pool fires.

ARTICLE INFO

Article history:
Received 17 October 2016
Received in revised form 5 June 2017
Accepted 6 June 2017

Keywords:
ASTEC-Na code
SFR containment benchmark
Sodium pool fire
Source term

ABSTRACT

Modeling the containment response to a sodium pool fire is to be one of the key aspects of any comprehensive safety evaluation of the new generation of sodium cooled fast reactors. Through a peer review of earlier experimental investigations some useful data can be collected and then used for assessing the current analytical capabilities to model severe accidents or some of their specific aspects. This paper provides major insights into the in-containment aerosol behavior predictability of ASTEC-Na (CPA* module) during Na-pool fires. By comparing against tests from the ABCOVE (AB1 and AB2) and FAUNA (F2) programs, it has been shown that experimental trends can be roughly reproduced with a single-cell approach whenever natural convection is effective in making the vessel atmosphere uniform both thermally and in composition. Nonetheless, the present heavy parametrization of ASTEC-Na models should be avoided or strongly supported by further experimentation that allows setting sound default values, concerning both combustion energy distribution and aerosol formation and distribution. Anyway, the peer data review has highlighted that a meaningful comparison to predictions is not always feasible due to large data uncertainties, particularly at the beginning of Na burning. As for the particle ageing, the comparisons set seems to indicate that transformation from oxides to hydroxides is predicted to be too slow; nevertheless, a more extensive benchmarking should be conducted to confirm it.

1. Introduction

The Gen. IV International Forum has, since the early 2000s, been exploring several different advanced nuclear reactor technologies that are supposed to offer enhanced safety, sustainability, and versatility over traditional nuclear reactor designs. Relying on past experience from the 1960s, 70s and 80s, the sodium fast reactor (SFR) is at the most advanced stage of the technologies that have been explored, with prototype reactors starting to come online, like the BN-800 reactor in Russia, or at an advanced stage in their design, like the ASTRID reactor concept in France.

Nuclear safety authorities in countries considering building Gen. IV technologies still have the responsibility to independently asses the proposed reactor designs. For SFRs, evaluating the effects of a sodium fire in containment would be an essential part of any safety evaluation because of how the fire can thermally damage the plant, cause an overpressure risk in containment, and be a source of airborne fission products as radionuclides dissolved in the sodium are aerosolized. Therefore, a full-scope SFR safety analysis demands validated computation tools capable of capturing the

* Corresponding author.
E-mail addresses: luisen.herranz@ciemat.es (L.E. Herranz), monica.gmartin@ciemat.es (M. Garcia), luke.lebel@irsn.fr (L. Lebel), fulvio.mascari@enea.it (F. Mascari), Claus.Spengler@grs.de (C. Spengler).

http://dx.doi.org/10.1016/j.nucengdes.2017.06.010
0029-5493/

Nomenclature

BC	Base case
BE	Best estimate
c_t	Thermal accommodation coefficient
F_{slip}	Particle slip coefficient
k_{gas}/k_p	Ratio of thermal conductivity of the gas over that for the particle
STICK	Particle sticking coefficient

Greek symbols

χ	Aerodynamic shape factor
γ	Agglomeration shape factor
ε	Turbulence dissipation rate
δ_{diff}	Diffusion boundary layer thickness
ρ	Aerosol density

main footprints of BDBAs in containment, so that Source Term estimates are considered reliable.

Although SFRs are being proposed as Gen. IV nuclear reactors, sodium fast reactors designs are not a new concept, and started to be investigated in parallel to light water reactors early in the nuclear era (IAEA, 2012). A vast amount of research and development was done from the 1960s to the 1980s, including the construction of different research, prototype, and demonstration reactions. With this, the development of analytical capabilities for source term analysis had to be carried out as well (Dunbar, 1985; Dunbar et al., 1984; Fermandjian, 1985). Most of the development of SFR technologies was abandoned in the 1990s with a general downturn in the nuclear industry; as a result, a lot of the expertise that was built previous decades has been lost. However, renewed interest in SFR technology is making the work done a generation ago extremely valuable, and there is a lot of rich experimental work and empirical model development that can be re-applied to evaluations of in-containment accident evolution in SFRs (Brunett et al., 2014; Herranz et al., 2013a,b; Spengler and Reinke, 2016). The EU-JASMIN project (Girault et al., 2015), for instance, has devoted a good fraction of their resources to develop and validate models in the domain of in-containment aerosols. As a consequence, a new version of the ASTEC module addressing in-containment accident evolution, hereafter denoted as CPA*, has been built by including models for sodium fires coming from SOFIRE (Beiriger et al., 1973) and models of chemical ageing of sodium-oxides particles, which were genuinely produced within the project (Mathe et al., 2015).

Beyond model development and implementation, qualification of any safety tool requires validation against a reliable and representative database. The present paper shows the results obtained in a benchmark set between ASTEC-CPA* and a number of experiments chosen from the open literature: ABCOVE-AB1, -AB2 and FAUNA-F2. These tests, conducted decades ago, investigated the anticipated pool fire scenarios during SFR severe accidents in large-scale vessels. Additionally, other codes have also been run so that modeling progress of ASTEC-CPA* can be also assessed with respect to other codes, like ASTEC-CPA, MELCOR, CONTAIN or SOPHAEROS-FEUMIX. It should be underlined that it is not the intention of this paper to discuss discrepancies among code estimates, but highlight the current predictability with the focus on CPA* behavior.

2. Selected experiments

An initial literature review of experimental information (Herranz et al., 2012) led to nearly 20 experiments related to Na fires, of which nearly half dealt with aerosol generation from pool fires. Not all of this work can be applied in this study, because they often investigate the dynamics of the pool and burning rates, rather factors important for this study, such as combustion product aerosolization and the thermal-hydraulic response of the containment volume. Likewise, working with these past experiments is often difficult, since copies of the original reports are often very difficult to obtain, and even then, data can often be incomplete or must be digitized from original plots. This is compounded by the fact that, since the work was conducted 30–40 years ago, the original investigators would have long since retired or passed away. Three of the 20 experiments identified in Herranz et al. (2012) were chosen for the benchmark purpose based on a number of criteria like their scale, completeness and accuracy of data reported and some others. As a result, attention was paid to specific tests of the ABCOVE and FAUNA programs, a succinct description of which is given below.

The ABCOVE experiments were conducted in the Containment System Test Facility (CSTF) vessel at the Hanford Engineering Development Laboratory in the United States. The containment was a cylindrical steel vessel (7.6 m diameter, 20.3 high) of about 852 m^3 (Fig. 1). The vessel was equipped with instrumentation to monitor both thermal-hydraulics and aerosol behavior. In these tests, the experimental arrangement included ten clusters of filter samples at various locations throughout the vessel atmosphere, each cluster containing 12 filters; four thief sample stations: the

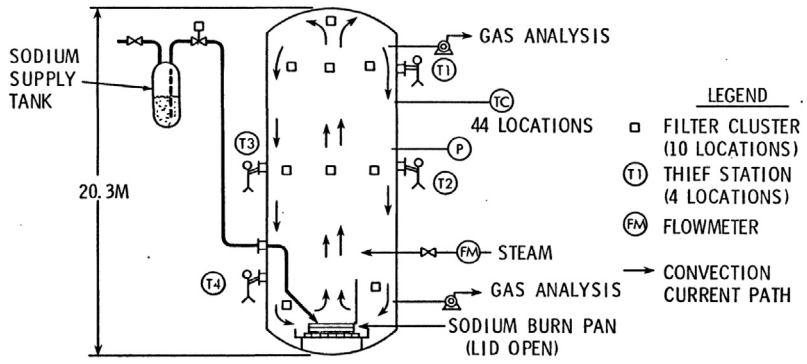

Fig. 1. CSTF vessel arrangement (Hilliard et al., 1977).

types of samples taken included filter samples for mass concentration measurements, samples for chemical species identification, deposition coupons and cascade impactors for particle size measurements; and two gas sample systems that provided on-line analysis of oxygen, moisture and hydrogen concentration (one taking gas from high in the atmosphere and one from low in the vessel). A more thorough description of experimental aspects may be found in Hilliard et al. (1979, 1977), McCormack et al. (1978), Souto et al. (1994).

The ABCOVE program conducted a total of 7 experiments related to Na fires and airborne aerosols, but only three of them were pool fire experiments (AB1, AB2 and AB7). Unfortunately, an experimental artifact in the AB7 execution prevented its use for validation purposes.

In test AB1, 410 kg of sodium at 600 °C was spilled into a burn pan of 4.4 m^2 through an electrically heated delivery line. The burn pan had a hinged lid which was in the vertical position during the spill. The sodium flow lasted 80 s and the splashing was minimized by baffles in the pan. At 60 min after the initiation of the spill, the lid was closed and the sodium pool fire extinguished.

The AB2 test was performed with essentially the same initial conditions, but with the addition of an injection of steam, at a rate of 0.02 kg/s, near the center of the containment vessel for 60 min beginning 16 min after the start of the fire. The steam injection was meant to simulate the release of water vapor from heated concrete at a rate equivalent to the release of water vapor from ~10 to 30 m^2 of hot concrete (at a ratio of 1.0 kg H_2O per kg of aerosol). In this test, 472 kg of sodium at 600 °C were delivered and the pool fire burn duration was 60 min.

FAUNA tests were conducted in the Kfk Laboratory for Aerosol Physics and Filter Techniques (LAF I) in Karlsruhe (Germany). The FAUNA facility consists of a fire room, a measuring room, and an aerosol measuring loop. A cylindrical steel vessel of 6 m in diameter and 6 m high with domed ends (volume 220 m^3) served as the fire room (Fig. 2) with all the instrumentation needed to monitor both thermal-hydraulics and aerosol behavior. Inside the FAUNA containment vessel, sodium pool fire was produced in a circular burning pan. Closely above the burning area a hood was placed in order to draw aerosols into the measurement loop. At these sample ports mass concentration of aerosol was determined by filter probes and size distribution by impactors. Additional filter probes were taken for the wet chemical analysis (Cherdron et al., 1990; Cherdron and Charpenel, 1985; Cherdron and Jordan, 1983, 1980).

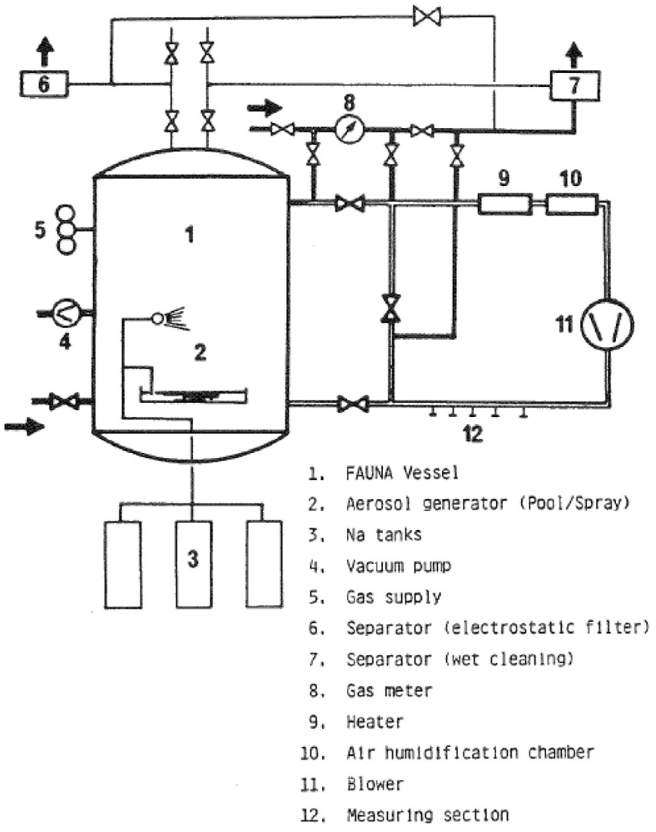

Fig. 2. FAUNA aerosol loop (Cherdron et al., 1985).

A total of 13 tests were conducted in the FAUNA facility, 7 of which (F1-F7) investigated pool fires. The F2 test was chosen to complete the set of experiments to be used in the benchmark due to the different scale compared to ABCOVE, the thorough reporting of data and the absence of any kind of experimental artifact that might affect results.

In the F2 test, a sodium pool fire was produced inside the FAUNA containment in a circular burning pan of 1.6 m diameter (~2 m^2) by the release of 250 kg of sodium at 500 °C for more than 3 h (210 min). During the experiment, the oxygen content was kept constant through 3 injections of approximately 1% of the vessel molar content with different duration.

3. Modeling of the experiments

As said above, in addition to the updated containment module of ASTEC, CPA*, other codes have been used: MELCOR 2.1, CONTAIN, SOPHAEROS-FEUMIX and, even the LWR version of CPA conveniently adapted. Table 1 matches codes and organizations responsible for their use. This benchmarking exercise was carried out as part of the JASMIN program, and included code-to-code comparisons partly because the set of suitable validation experiments is fairly small, and partly to assess some of the code prediction uncertainty and user-effects. Four organizations have participated: CIEMAT, GRS, IRSN, and ENEA.

3.1. Codes description

ASTEC (Klein-Hessling and Schwinges, 1998) and MELCOR (Gauntt et al., 2005) are fully integrated engineering level computer codes that model the progression of severe accidents in LWRs. In both, aerosol modeling is based on the MAEROS code (Gelbard, 1982), a multi-section, multi-component aerosol dynamics code that assesses the evolution of particles size distribution of each type of aerosol defined.

ASTEC-Na (Girault et al., 2015) is a new computer code system that is currently being developed to model severe accidents in SFRs. Based on ASTEC modules platform, this code is being adapted to SFR accident environments. In particular, a new version of CPA module (CPA*) is now available to predict the in-containment source term during a sodium pool fire. Two new models have been implemented into the CPA* module of ASTEC-Na as part of this development effort: (i) a model based on the SOFIRE-II model (Beiriger et al., 1973) to account for the heat and aerosol emissions

Table 1
Codes and organizations.

	CIEMAT	ENEA	GRS	IRSN
ASTEC-CPA		x		
ASTEC-CPA*	x		x	
CONTAIN			x	
FEUMIX_SOPHAEROS				x
MELCOR		x		

from a sodium pool fire, and (ii) a chemical transformation model that calculates reactions of the sodium-oxide aerosols with steam and CO_2 in the atmosphere.

CONTAIN (Murata et al., 1997) is a modular and integrated analysis tool used for predicting in-containment source term after a severe accident. The models for the aerosol behavior implemented in CONTAIN are based on the stand-alone aerosol code MAEROS. In this code, the modeling of sodium pool fires is also based on the SOFIRE-II models (Beiriger et al., 1973).

FEUMIX is an SFR containment thermal-hydraulics code designed to calculate the thermal consequences of an accidental sodium leak and the resulting jet fire or pool fire that could occur (Jacq and Lefévre, 1995). As FEUMIX does not have the capability to model aerosol dynamics, FEUMIX results are externally coupled with ASTEC-SOPHAEROS code in order to compute the evolution of the airborne aerosol concentration, aerosol size distribution and wall deposition rates.

3.2. Nodalisation and heat structures

3.2.1. ABCOVE Nodalisation

All the AB1 and AB2 calculations share the same nodalisation: a single cell (852 m^3). Six walls for the heat transfer and aerosol deposition representing the top and bottom heads, the cylindrical wall, the internal components for aerosol plating and settling and the sodium pool surface, have been considered in CPA*_GRS, CPA*_CIEMAT, CONTAIN_GRS and FEUMIX_IRSN simulations; the same is defined in CPA_ENEA and MELCOR_ENEA simulations but a wall representing the personnel deck has been added. The surface areas and their orientation are given in Table 2. A noticeable discrepancy exists concerning the vertical internal wall surface among the codes; the reason for it is that CPA*_GRS, CONTAIN_GRS and FEUMIX_IRSN have limited those surfaces areas to those involved in heat exchange, whereas the rest of codes have considered those surfaces involved in aerosol deposition.

In all the cases, the surface material facing the vessel atmosphere has been stainless steel (2.29 cm). At the outer surface, some calculations defined a 2.54 cm layer of fiberglass, as used in the facility; nonetheless, not quite the same properties have been used by ENEA and CIEMAT: 753 vs 795 J/kg·K as specific heat; 0.0467 versus 0.047 W/m·K as conductivity; and 96 vs. 220 kg/m^3, as density. From the outer side of the insulation to the environment natural convection has been assumed in some cases (CPA_ENEA, CPA*_CIEMAT and MELCOR_ENEA). An adiabatic condition from the stainless steel to the environment has been imposed by others (CPA*_GRS, CONTAIN_GRS and FEUMIX_IRSN).

The sodium pool surface is modeled as a 4.4 m^2 hot structure facing the gas atmosphere in most calculations, except for CONTAIN_GRS and FEUMIX_IRSN ones, which have assumed a sodium liquid surface of the same dimension.

3.2.2. FAUNA nodalisation

The nodalisation of the FAUNA vessel has been essentially the same for all the calculations. Again, only one node has been used (220 m^3) in all the calculations. Four walls (top and bottom heads, cylindrical wall and sodium pool) have been considered for heat transfer and aerosol deposition. Table 3 shows the surface areas and their orientation. As in the case of CSTF, some calculations have assumed the entire surface area of the bottom head, whereas others have assumed just the cross section of the vessel cylinder (i.e., heat-exchange surface area or particle-deposition surface area).

The vessel walls (top, bottom and cylinder walls) have been modeled as stainless steel (1.6 cm thick). As no accurate information on the vessel insulation has been found, thermal insulation is simulated imposing adiabatic conditions at the bottom head and constant external temperature (80 °C) at cylindrical walls and upper head. As in the ABCOVE models, sodium pool has been modeled as a rigid structure (2 m^2) by most modelers, except for

Table 2
Nodalisation overview (CSTF vessel).

CSTF vessel	CPA*/CONTAIN (GRS)	CPA* (CIEMAT)	CPA/MELCOR (ENEA)	FEUMIX (IRSN)
Nodalisation (nodes n°)	1	1	1	1
HS				
N° of HS	6	6	7	6
HS(m^2)/Orient	-Bottom (63)/H -TopHead (63)/H -CylWall (394)/V -Hor_Int(36.2)/H -Vert_Int(184.8)/V -Na pool (4.4)/H	-Bottom(45.60)/H -TopHead(63)/H -CylWall (395)/ V -Hor_Int(42.7)/ H -Vert_Int(232)/ V -Na pool (4.4)/H	-Bottom (45.58)/H -TopHead (63)/H -CylWall (395)/V -Hor_Int(36.2)/H -Vert_Int(232)/V -Na pool (4.4)/H -Pers_Deck(10.5)/H	-Bottom (63)/H -TopHead (63)/H -CylWall (394)/V -Hor_Int(36.2)/H -Vert_Int(184.8)/V -Na pool (4.4)/H

Table 3
Nodalisation overview (FAUNA vessel).

FAUNA vessel	CPA* (CIEMAT)	CPA/MELCOR (ENEA)	FEUMIX (IRSN)
Nodalisation (nodes n°)	1	1	1
HS			
Number of HS	4	4	4
HS(m^2)/Orient.	-Na pool (2)/H -Bottom (28.3)/H -TopHead (31.5)/H -CylWall (113)/V	-Na pool (2)/H -Bottom (31.5)/H -TopHead (31.5)/H -CylWall (113)/V	-Na pool (2)/H -Bottom (19.5)/H -TopHead (31.5)/H -CylWall (113)/V

FEUMIX_IRSN in which sodium pool has been explicitly modeled as a sodium liquid surface of identical dimensions.

3.3. Major hypotheses and approximations

Even though, generally speaking, most simulations share a similar approach, there are some differences that led to some results differences and are worth highlighting:

- Natural convection regime has been set to describe gas-surface exchanges. As for thermal radiation, most calculations have taken it into account; GRS, though, has assumed that high aerosol loading of vessel atmosphere would prevent radiation from being effective.
- Heat transfer between Na pool and atmosphere has been approximated differently. CPA*_GRS, for instance, has assumed a constant temperature of Na (1150 K) and a given heat transfer coefficient of 25 $W/m^2 \cdot K$ during fire duration based on previous analyses by other authors (Scholtyssek and Murata, 1993). Instead, other calculations like CPA*_CIEMAT, CPA_ENEA and MELCOR_ENEA, left the calculation to be done without any restriction other than an emissivity setting for Na thermal radiation. CONTAIN_GRS considers a special set-up of boundary condition to provide consistency with the assumption of a constant sodium pool temperature, like in CPA*_GRS; in this case, the lower pan surface temperature is imposed and heat is conducted up to the upward pool surface.
- Combustion energy magnitude and distribution are essential ingredients of the models. Several codes share the "SOFIRE-II" approach: two parameters defining the fraction of oxygen producing Na_2O (f_1) and the fraction of the chemical energy absorbed by the Na pool (f_2), are given. GRS settings are based on past studies with CONTAIN (Langhans, 1991); CIEMAT has assumed that Na_xO_y formation reactions are infinitely fast (f_1) (i.e., both oxide and peroxide formation reactions are supposed to reach equilibrium instantaneously); a rough estimation of the ratio between the heat flux by radiation from the flame to the pool surface and the heat flux by convection from the flame to the ambient, supports the f_2 choice; consistently with the absence of *ad-hoc* models for Na combustion in CPA and MELCOR, ENEA's settings for f_2 are those that best match the Peak Containment Atmosphere Temperature (PCAT); finally, FEUMIX includes Na pool combustion models and it just considers Na_2O as the resulting species, so that it does not require those f_i parameters. Table 4 collects the values assumed by different participants.

Besides these generic aspects, some test specifics are dealt with differently. According to the AB2 experimental conditions, a steam mass rate of 0.019 kg/s is injected from 960 s to 4560 s in CPA*_GRS, CPA*_CIEMAT, CONTAIN_GRS and FEUMIX_IRSN calculations. As chemical reactions are not calculated by CPA and MELCOR codes, no steam is injected in CPA_ENEA and MELCOR_ENEA calculations.

Concerning the oxygen supply in the F2 test during the experiment, the injection was switched on/off to keep the oxygen concentration roughly constant over the test duration (between 15 and 25%). Accordingly, an injection of oxygen during the sodium pool fire phase has been defined in CPA*_CIEMAT calculation (0.005 kg/s between 0 and 6000 s and 0.006 kg/s between 6000 and 12,000 s). In FEUMIX_IRSN, an oxygen injection that linearly varies between 0.013 kg/s and 0.007 kg/s has been employed. Oxygen supply has not been considered in CPA_ENEA and MELCOR_ENEA F2 calculations.

3.4. Aerosol modeling

CPA* new models estimate the amount of Na_2O and Na_2O_2 particles formed along time (the same is applicable for CONTAIN and FEUMIX). Nevertheless, the amount that eventually enters the atmosphere of each species is determined through the f_3 and f_4 parameters in the input deck (Table 5). CIEMAT settings have been defined to get the best fit to data, whereas GRS's assume that all Na_2O get instantaneously depleted on surfaces (i.e., no Na_2O in the atmosphere), which seems to be consistent with experimental observations concerning Na aerosol composition (Hilliard et al., 1979).

Unlike the codes mentioned above, CPA and MELCOR need to define an aerosol injection rate. Then, in CPA_ENEA and MELCOR_ENEA calculations, an aerosol source is imposed as a constant mass flow rate lasting during the Na burning;; the rate has been set from the experimental observations at the end of Na burning (Table 6).

Particle size distribution is one of the main characteristics governing aerosol behavior. The way the codes deal with it is diverse:

Table 5
f_3 and f_4 values.

	CPA* (GRS)	CPA* (CIEMAT)	FEUMIX (IRSN)
AB1/AB2 tests			
f_3	0.0	0.25	0.22
f_4	0.5	0.25	–
F2 test			
f_3	*	0.00	0.22
f_4	*	0.10	–

f_3: fraction of Na_2O released in the atmosphere (complement is released in the pool).
f_4: fraction of Na_2O_2 released in the atmosphere (complement is released in the pool).
* Non-participant.

Table 6
Aerosol mass flow rate (kg/s) in CPA_ENEA and MELCOR_ENEA calculations.

TEST	CPA/MELCOR
AB1	0.0111*
AB2	0.0107*
F2	0.00128**

* From Hilliard et al. (1979).
** From Cherdron et al. (1990) and Cherdron and Jordan (1980).

Table 4
f_1 and f_2 values (for AB1, AB2 and F2 tests).

	CPA*/CONTAIN (GRS)	CPA* (CIEMAT)	CPA (ENEA)	FEUMIX (IRSN)	MELCOR (ENEA)
f_1	0.3	0.33	–	–	–
f_2	0.7	0.5	0.54	–	0.56

f_1: fraction of oxygen consumed to produce Na_2O (complement is used for Na_2O_2 formation).
f_2: fraction of the reaction energy released in the pool (complement is released in the atmosphere).

in some codes, primary particle size has been used as the basis for the initial MMD of the distribution and then allow particles to agglomerate (CPA*, CONTAIN and FEUMIX), while in others (MELCOR and CPA), the specified MMD comes from an already agglomerated particle distribution and it is based on available experimental data. Anyway, a lognormal distribution has been assumed in all the cases. Table 7 collects the initial MMD (Mass Median Diameter) and GSD (Geometric Standard Deviation); note that italics have been used when the code internally calculates the variable.

Additionally, some other particle features are often set in the input deck (i.e., shape factors, conductivity, sticking efficiency, etc.). Table 8 gathers the different code assumptions. Generally speaking, code default values have been used. Some variability exists, though, in density: whereas GRS and CIEMAT estimated it as a function of Na_2O and Na_2O_2 distribution, as described by f_1; ENEA took the estimated aerosol material density for the AB1 test (Hilliard et al., 1979). IRSN just set the Na_2O density, as it is the only species formed in FEUMIX.

In CPA* an ageing model to evaluate the aerosol chemical reaction with steam and CO_2 in the atmosphere has been implemented (Mathe et al., 2015). In this model, the Cooper diffusion coefficient must be defined by the user. In both calculations with CPA* (CPA*_GRS and CPA*_CIEMAT) a value of $5{\cdot}10^{-9}\ m^2s^{-1}$ is used (Mathe et al., 2015). In FEUMIX, the production of Na_2O_2 is not considered as it is assumed that only Na_2O is produced. However, FEUMIX is able to calculate the reaction between the aerosol-phase Na_2O and water vapor in the containment atmosphere to produce NaOH, by assuming a fast, binary gas phase reaction with a rate constant of $10^5\ s^{-1}$.

4. Results and analysis

In order to suitably focus the results analysis, some previous discussion on the data used for comparison is indispensable. Two key aspects of the data are: the local/average nature and the source from which the data have been withdrawn. The local/average nature is directly related to their significance as a footprint of the whole scenario (as local values of some variables could not give a meaningful hint of the governing phenomena) and to the credit that data-estimates comparisons should be given in terms of validation (i.e., comparison of a local gas temperature with the gas temperature prediction of a single node calculation for a vessel of hundreds of m^3 might be meaningless). The uncertainty associated to the data withdrawal process can be crucial: a numerical value taken from a text or table in a scientific/technical report can be assumed to be "as given", whereas if data are taken from figures the withdrawal accuracy will be dependent on the quality of the plot, the type (linear vs. log), the tool used to pick the data points, etc.

4.1. Thermal-hydraulics

4.1.1. Data analysis

In the AB1 and AB2 tests, the experimental temperature is the mean value of thermocouples from high, low and central regions in the containment atmosphere at different azimuthal locations and distances from the center. According to Hilliard et al. (1979), the maximum standard deviation of average temperature of 8 thermocouples located at different positions in the vessel is below 5% in both tests (as shown in the figures below). All the values have been taken from tables, so no error should be attributed to the data withdrawal process. In short, everything seems to indicate that data-predictions comparison can be set and given credit whenever the experimental errors are taken into account.

As for pressure, any local measurement can be reliable for comparison with single-cell estimates and no error has been made in the withdrawal process since data have been taken as numerical values from a table.

In the F2 test, the two local temperatures at the same axial location (around 4 m above the pan base) and the two radial positions that cover all the local measurements have been considered for comparisons. Given the shortage of information at other locations, particularly at different heights and radii, the comparison to a "cell temperature" estimated by codes should be done in terms of trends and order of magnitude. Additionally, some errors should be associated to the withdrawal process as data were taken from a figure (Cherdron et al., 1990) in which the broad scale in temperatures and time would allow absolute errors of 10 K and 60 s, respectively.

4.1.2. Codes predictions

Atmosphere temperature and pressure for AB1 and AB2 tests are shown in Figs. 3 through 6. From the experimental data, gas

Table 7
MMD and GSD (for all the tests).

	CPA*	CONTAIN	FEUMIX	MELCOR/CPA (AB1-2/F2)
MMD	$\sim 1{\cdot}10^{-9}$ m	$\sim 1{\cdot}10^{-9}$ m	$1{\cdot}10^{-9}$ m	$1{\cdot}10^{-6}$ m/$0.89{\cdot}10^{-6}$ m
GSD	2.0	2.0	2.0	2.0*/1.4**

* From Hilliard et al. (1979).
** From Cherdron and Jordan (1980).

Table 8
Aerosol coefficients and density (for all the tests).

	CPA*	/CPA	CONTAIN	FEUMIX	MELCOR
χ	1.00	1.00	1.00	1.00	1.00
γ	1.00	1.00	1.00	1.00	1.00
F_{slip}	1.37	1.37	–	–	1.257
STICK	1.00	1.00	–	1.00	1.00
ε	0.02	0.02	0.02	0.02	$1.00{\cdot}10^{-3}$
k_{gas}/k_p	0.03	0.03	0.03	0.04	0.05
c_t	1.00	1.00	–	–	2.25
δ_{diff} (m)	–	$1.00{\cdot}10^{-4}$	$1.00{\cdot}10^{-5}$	–	$1.00{\cdot}10^{-5}$
ρ (kg/m^3)	2800	2420	2800	2270	2420

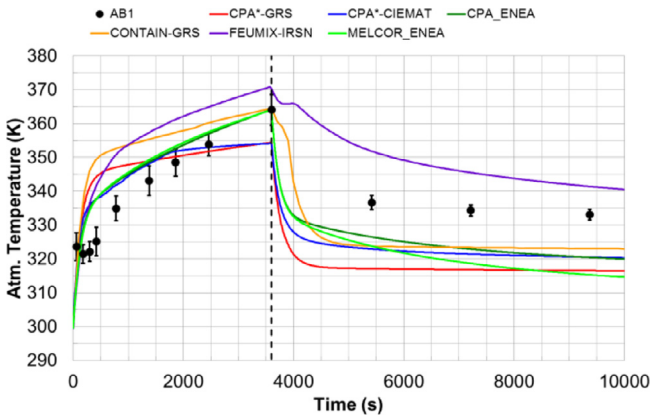

Fig. 3. Average atmosphere temperature (AB1).

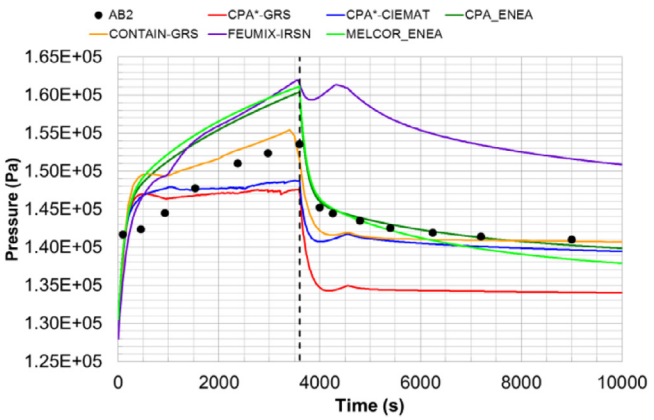

Fig. 6. Pressure (AB2).

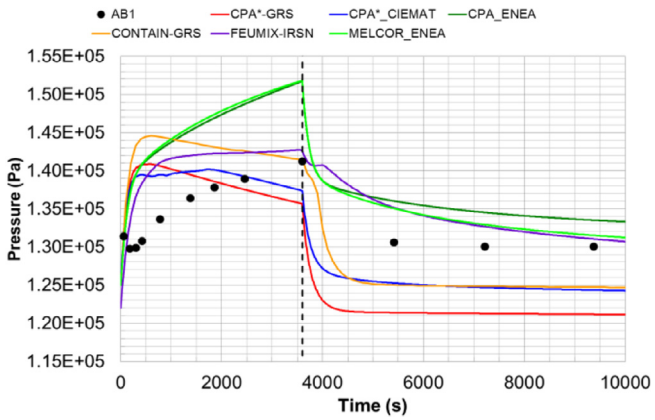

Fig. 4. Pressure (AB1).

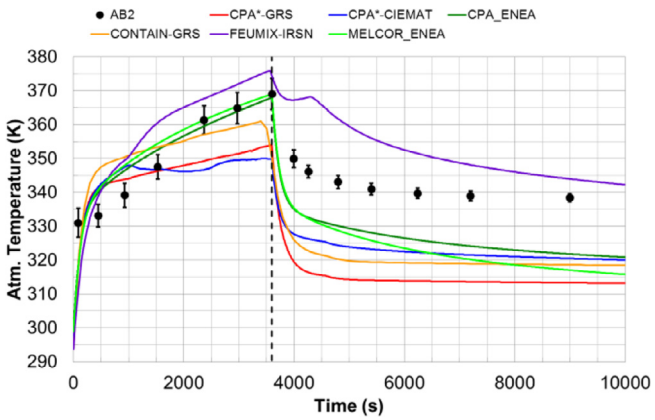

Fig. 5. Average atmosphere temperature (AB2).

temperature evolution may be described in two main phases: heat-up and cool-down. The heat-up phase is, in turn, split into 4 stages: a first period (about 60 s) in which a sharp increase of temperature occurs; a second one along which temperature hardly changes for about 500 s; a third one in which temperature increase proceeds gently for some 2000 s; and a last period until the fire quenching, where heat-up slightly slows down.

An explanation of the profile described above can be postulated. Na pouring into the experimental pan entails a large surface-to-volume ratio of so-called "fresh Na", which is eager to react without any major kinetic resistance than the one associated to O_2 availability (note that "fresh Na" becomes available in a continuous way). Contrarily, once in the pan, several factors might slow down the chemical interactions: Na surface/volume ratio is notably less and some kinetic resistance for Na-O_2 interaction can be anticipated regardless it develops as a surface reaction (i.e., O_2 should diffuse into the pool bulk) or as a gas reaction (Na vaporization would take also some time); some of the Na thermal energy would be absorbed by the pan until reaching the Na-pan thermal equilibrium, which in turn would slow down Na vaporization rates and, as a consequence, gas Na-O_2 reactions would take longer to start up; finally, there might be a sort of "incubation period" until natural convection currents set up at full intensity in the scenario. In between these two different oxidation regimes, there is a transition period that reflects the time gap necessary to reach a sort of steady oxidation rate of "in-pan" Na.

The cool down period shows two steps: a fast one due to chemical reactions brought to a halt and the isolation of the hot sodium by covering the burn pan, and a longer and more progressive one, as heat is steadily lost to the vessel walls by natural convection.

Consistently with major experimental observations, calculations also show the two main experimental phases. However, differences show up when focusing in each of them. On one side, only two periods are predicted in the heating phase and, regardless if they match the maximum temperature at the end of the phase, all in all measured heating rates are poorly captured, except for those calculations corresponding to "fitting-to-PCAT-data" approaches (i.e., CPA/MELCOR_ENEA). This is not surprising as none of the models took into account the Na-injection effects discussed above and set key parameters (f_1 and f_2) on arbitrary basis requiring validation. On the other, cooling rate due to fire quenching is largely overpredicted at the beginning of the cooling phase, which might indicate too high of an energy source during the fire period (0–3600 s); in the longer cooling period there are also deviations but they are not as noticeable as those discussed above.

The two major points discussed in the previous paragraph are also applicable in F2 analysis (Fig. 7). Nonetheless, according to thermocouples located at different heights in the vessel (x = 0.0 m and x = 3.0 m) F2 atmosphere was not well mixed during Na burning. In addition, temperature at x = 0.0 m is highly sensitive to O_2 concentration, so that whenever O_2 concentration decreases temperature falls down quite noticeably. Finally, even though the end of fire is set to be at 12600 s in the test protocol, according to temperature records, fire started extinguishing progressively since around 6000 s. As O_2 concentration is far from being zero in the vessel at 6000 s, the temperature trend might mean that it takes some time for O_2 at other locations than the burning pan vicinity to reach it or, in other words, that Na burning is much

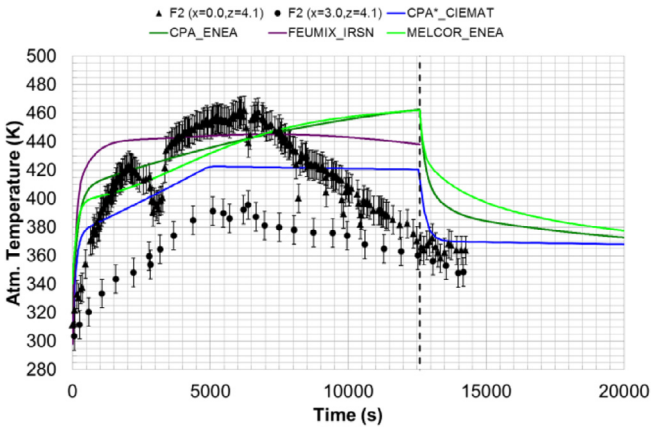

Fig. 7. Atmosphere temperature (F2).

faster than convection loops set in the vessel as a consequence of Na burning. This experimental footprint is not captured by predictions, in which fire end were set to happen at 12,600 s.

From the above discussions one may withdraw some take-aways from the modeling perspective:

- Energy source into the gas atmosphere during Na pool burning should be further investigated, so that models are based on a sort of mechanistic understanding instead of on empirical, and sometimes arbitrary, settings.
- The single-node approach seems to be capable of following data trends under soft transients; however, under fast transient conditions driving to atmosphere non-uniformity for a while, such an approach looks unable to follow observations and significant deviations would occur.

4.1.3. Codes intercomparison

Thermal-hydraulic vessel conditions are mostly governed by the amount of energy released to the atmosphere during the sodium pool fire (Na-oxygen reactions). In the next table (Table 9) the integral energy released to the atmosphere due to combustion is shown for the AB1 test: the calculated energy by CPA* and CONTAIN code and the user defined energy injection in CPA and MELCOR codes. Note that the energy released to the atmosphere as given in Table 9 is calculated as the fraction of the total combustion energy delivered to the atmosphere, which is given by the parameters f_1 and f_2. As it can be observed, quite similar values of the combustion energy are predicted in all the simulations.

The differences among codes might lie on the distribution of the energy released between pool/atmosphere and the different approaches for sodium pool heat transfer. In CPA*_GRS, an added heat transfer coefficient of 25 W/m^2·K in the sodium pool structure is assumed. This provides a power of about 100 kW which along with the combustion power injected to the atmosphere (166 kW, Table 8) result in an overall power of 266 kW. In CPA*_CIEMAT calculation, radiation from the pool has been modeled (about 85 kW during the sodium pool fire) and as the power by combustion is bigger than CPA*_GRS one (195 kW, Table 9), finally both calculations predict almost the same overall power which result in a very similar atmosphere temperature prediction. In ENEA calculations, assuming a radiation power similar to CIEMAT's, the atmosphere temperature increase discrepancy, between the two calculations, is explained by the significantly larger combustion power assumed (220 kW for MELCOR and 230 kW for CPA, Table 9). Regarding the larger overestimation of the temperature increase in the very first phase of CPA*_GRS calculation, it is likely due to the assumption of 25 W/m^2 K during the sodium pool fire. In CPA*_-CIEMAT, however, at the beginning of the sodium pool fire, the heat transfer coefficient by radiation is about 6 W/m^2·K, which gives a smaller temperature increase.

After the fast heat up phase predicted by the codes, a milder slope is observed in CPA* and CONTAIN calculations which is referred to the decreasing burning rate in contrast to the ENEA calculations (in which constant average burning rate is assumed). CONTAIN has the capability to simulate the heat up of the sodium pool, but in CONTAIN_GRS calculation a similar behavior as in CPA* is forced by the approximations made. Similar trends can be observed among CPA_ENEA, FEUMIX_IRSN and MELCOR_ENEA calculations during this phase.

Because of the thermal insulation of the outer vessel surface the long-term atmosphere temperatures after end of pool fire are determined by the heat-up of the structures and their long term surface temperature. Some differences among codes can be observed. Between CPA*_GRS and CPA*_CIEMAT discrepancies are mainly due to the different approaches for the sodium pool as a wall: a constant temperature is assumed in the first one while an evolving temperature is allowed in the second one. The higher temperature of CONTAIN_GRS compared to CPA*_GRS is explained because of similar but non-identical thermal behavior of the sodium pool (and thus larger heating of the atmosphere by CONTAIN). FEUMIX_IRSN calculation, on the other side, is not able to capture the fast cool down phase: there is no means in the code to isolate the hot sodium pool from the rest of the containment volume, as was done in the AB1 experiment. It is worth noting that due to the hypothesis assumed concerning sodium pool surface heat transfer, the code's predictions during the depletion phase (i.e., pool fire over) must be cautiously taken.

The experimental gas temperature evolution in AB2 test is the same as for the AB1 test. The ascending trend during the Na injection phase is roughly captured by most predictions (except for CPA*_CIEMAT, in which the steam injection effect is noticeable), although curve slopes deviates from measurements. The closer-to-data code estimates are those of CPA_ENEA and MELCOR_ENEA during the Na injection phase, particularly after 2000 s. Anyway, the major deviations have been observed during the cooling phase, as most codes estimates a much faster cooling than recorded (except for FEUMIX that predicted a slower cool down at the beginning of the phase). Generally speaking, the codes are capable to follow the data trends, but significant differences can be noted during both the ignition phase (10–25 K) and the cool-down period (10–40 K).

Atmosphere temperature for F2 test is shown in Fig. 7. As in the case of the ABCOVE simulations, codes estimate a fast increase at the beginning of the test; data, however, show a slower temperature increase, even at locations near the Na pool. Nonetheless,

Table 9
Integral energy of combustion injected into the atmosphere (J) (AB1 test).

	CPA* (GRS)	CPA* (CIEMAT)	CPA/MELCOR (ENEA)	CONTAIN (GRS)
AB1				
Energy	5.43·10^8	7.01·10^8	(1-F)·1.80·10^9	5.47·10^8
Mode	Code	Code	User	Code

what is specific of F2 is the codes failure to capture the decreasing trend observed from 6000 s up to the end of the fire (12,600 s). As said above, this is probably related to the non-well mixed atmosphere, contrary to what was assumed in the codes modeling, and the drastic Na-burning slow down at 6000 s that might have been caused by a limitation in the O_2 supply to the Na pool region. The different trends between CPA*_CIEMAT calculation and CPA_ENEA, MELCOR_ENEA calculations, might well be because of an assumed constant burning rate that gives off an increasing monotonic temperature.

Regarding gas pressure in AB1 test, the overall experimental trends are followed by the CPA_ENEA, FEUMIX_IRSN and MELCOR_ENEA calculations but higher values are found; FEUMIX_IRSN predictions agree even better with the experimental data. However, inverse tendencies are found in CPA*_GRS, CPA*_CIEMAT and CONTAIN_GRS calculations. This inverse tendency is due to a higher gas species depletion due to the pool fire (i.e., O_2 burning) and the consumption of gaseous species during aerosol ageing. In the AB2 test, the gas species depletion in CPA*_GRS, CPA*_CIEMAT and CONTAIN_GRS pressure calculations is compensated to some extent by the steam injection, which prevents estimates from showing a decreasing trend as in AB1.

4.2. Aerosol behavior

A lot of aerosol related data were collected in the experiments. The three main metrics used in the code benchmarking exercise are the suspended mass concentration, the Aerodynamic Mass Median Diameter (AMMD), and the mass distribution at the end of the tests.

4.2.1. Data analysis

In the AB1 and AB2 tests, the experimental suspended mass concentration is the average of 4 locations from high, low and mid regions in the vessel and the data are available as tables in Hilliard et al. (1979). As noted in the figures below, the standard deviations at some times are substantial, so that any data-predictions comparison should be done with caution, particularly during the aerosol generation phase of the experiments.

The average AMMD measurements were taken at high and low containment locations and they show a noticeable consistency. It is noteworthy that the first data point available is around 1000 s, so that the time gap since the fast Na-injection transient has been long enough to reach a reasonable degree of uniformity in the vessel. Thus, from the aerosol perspective, any data-prediction comparison seems reasonable even under the well-mixed atmosphere hypotheses made in the calculations. Nonetheless, taking data points from a log-log plot results in withdrawal uncertainties that have been postulated to be dependent on the relative position of the data points with respect to the beginning of the order of magnitude (OM) in the log scale: 0.1·OM, if data are near the mark of the OM in the plot; and 1.0·OM, if data are closer to the next OM. This approximate way of estimating uncertainty ranges is the basis of the ones shown in the figures below.

The distribution of deposited sodium is taken from tables. According to these tables, only the deposited sodium on the bottom and the safety catch pan and personnel deck come from measurements. The rest of values are calculated (Hilliard et al., 1979).

For the F2 test, local measurements have been taken for both concentrations and AMMDs. Contrary to the ABCOVE tests, there is no experimental evidence that facility atmosphere was well-mixed, so any local magnitude cannot be taken as representative of the whole facility. In addition, concentration data points in the plot have been taken by selecting specific spots along a continuous curve in a log-log plot. As for uncertainties associated to data points, the same criteria as the ones defined above for ABCOVE have been used for concentrations, in which both axes are in log scale (Cherdron et al., 1985). AMMDs measurements were derived from samples taken closely above the burning area (i.e., approximately 200 s ageing), so that they cannot be said to be representative of particle sizes in the entire vessel; the data points have been taken from a linear–linear plot.

4.2.2. Codes predictions

Contrarily to the thermal evolution in the ABCOVE tests, aerosol evolution in AB1 and AB2 cannot be discussed together.

Fig. 8 shows the evolution of the aerosol concentration in AB1 test. It is worth noting the large uncertainties associated with the experimental data before 1000 s. During the burning phase (0–3600 s), a quasi-steady state between 0.02 and 0.03 kg/m^3 was measured, so that there was a balance between particle generation and aerosol deposition; afterwards, once the Na fire is over, concentration decayed progressively. Despite that some of the calculation results fall within experimental uncertainties during the quasi-steady state period, none of them follows the observed steady trend before the sodium pool fire ending. Besides, the experimental depletion rate during the first 1000 s of the depletion phase is about twice higher than the predictions.

Fig. 9 displays the AMMD evolution. The data experienced a jump from about 6 μm to approximately 8 μm between 4000 and 5000 s. This change is nothing to do with a sort of agglomeration enhancement, but it is the result of the end of injection of small particles from the fire, so that naturally the size distribution shifted to bigger sizes. Then, a progressive decrease of the particle size can

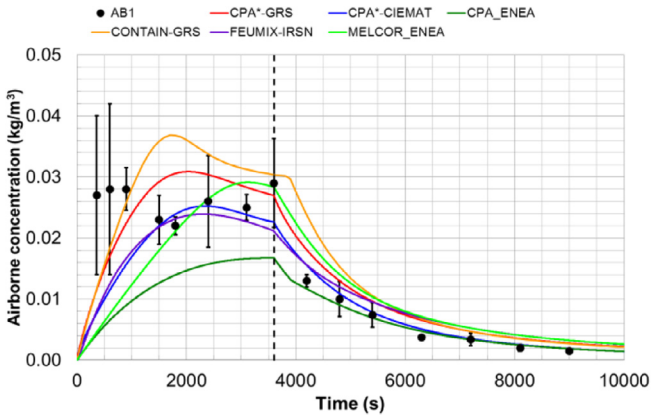

Fig. 8. Airborne concentration (AB1).

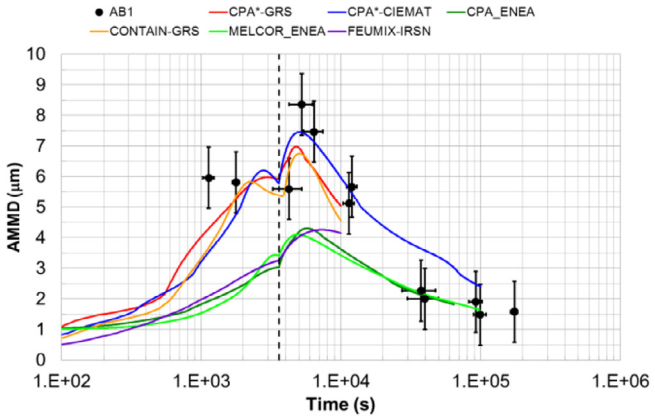

Fig. 9. AMMD (AB1).

be observed as a consequence of preferential deposition of large particles by sedimentation. Calculations cluster in two groups one of which reasonably follows measurements (CPA* and GRS), whereas the other (CPA, MELCOR and FEUMIX) noticeably underpredicts particle size until reaching about 40,000 s. Even though the reasons for this different behavior should be investigated further, the results seem to confirm the codes capability to capture particle size changes.

Fig. 10 shows the final mass distribution. Even though some tools got it qualitatively, still noticeable differences are noted in magnitude. In general, it seems that all the codes overestimate the importance of thermophoresis as a deposition mechanism, predicting a much higher mass fraction on walls and vertical surfaces than observed.

Again in AB2 (Figs. 11–13) it is not easy to identify a clear trend during the aerosol injection period (0–3600 s) due to the substantial uncertainties affecting some of the data. However, one may assume a soft growing trend from around 0.02 kg/m^3 to 0.035 kg/m^3. The depletion phase, although qualitative similar to AB1 one, shows an initial decay rate nearly 3 times slower. These variations with respect to AB1 make calculations resemble concentration measurements more closely. Anyway, the uncertainty associated to the data point at the end of the Na fire period might well be on the root of that difference.

Contrary to differences in AB2 concentration profile with respect to AB1, AMMD shows an evolution very similar to AB1, both qualitatively and quantitatively (Fig. 12), and calculations also behave the same way. Likewise, the main insights from the AB1 final mass distribution can be applied to AB2 (Fig. 13).

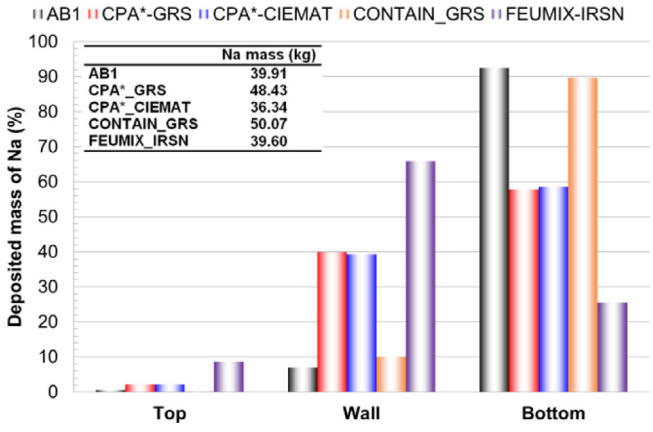

Fig. 10. Na mass distribution (AB1).

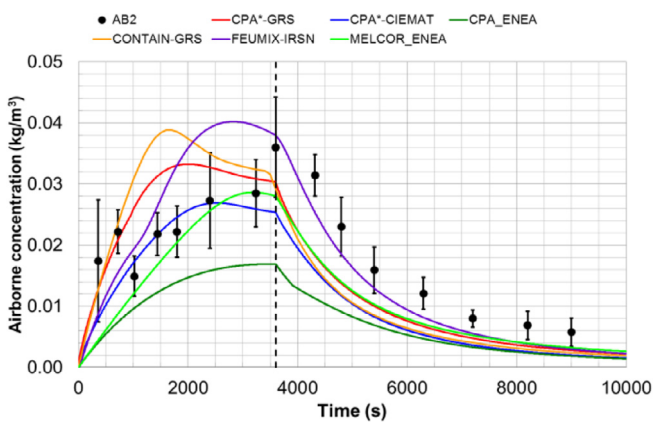

Fig. 11. Airborne concentration (AB2).

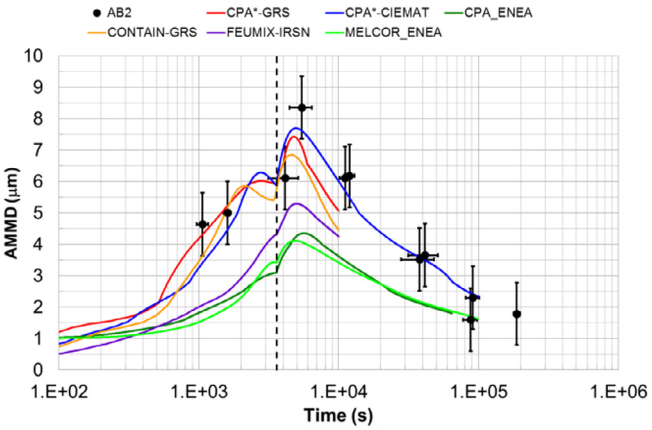

Fig. 12. AMMD (AB2).

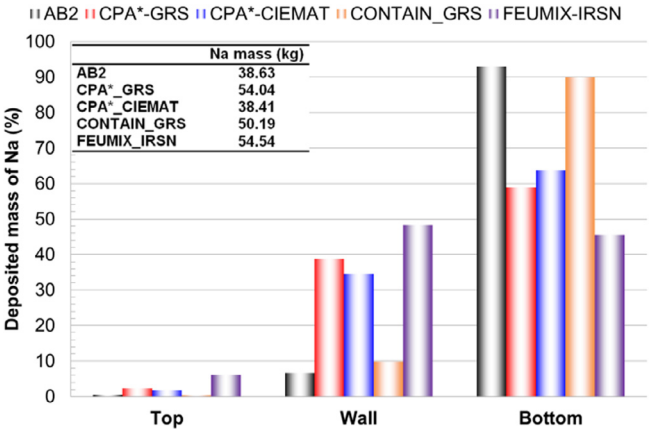

Fig. 13. Na mass distribution (AB2).

The evolution of the airborne concentration in F2 test is presented in Fig. 14. The first experimental data is approximately at 1000 s. From this time, experimental airborne concentration seems to draw a slow growth up to 6000 s and then an equally slow decrease, which is consistent with the thermal observations made above and the postulate of a reduced of Na-burning; however, when uncertainty bars are accounted for, such an experimental trend is harder to defend. As occurred with temperatures, calculations have not followed the described trends, but at least CPA* and

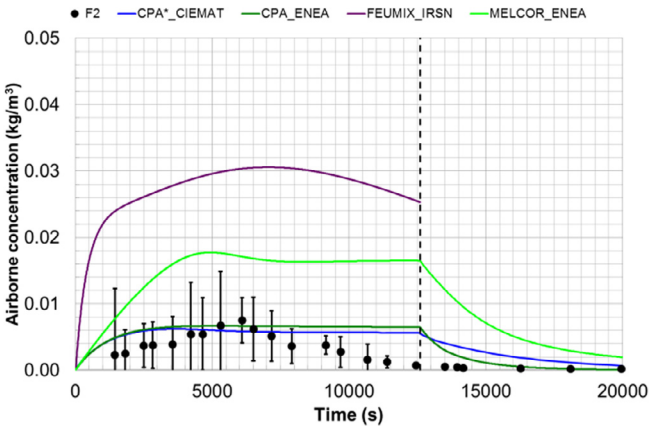

Fig. 14. Airborne concentration (F2).

CPA showed a steady concentration at a value close to the maximum data measured. However, given how data were taken, it is highly likely that measured concentration cannot be understood as an average concentration in the vessel.

Regarding the particle size (Fig. 15), as data were taken quite close to the aerosol source, overpredicting should be the expected code behavior, as particles with short time of flight would not have had the time to agglomerate to a good extent. Nonetheless, in generic terms data and calculations are around similar a value of 2.0 μm. Again, it is highly likely that this comparison is unsuitable.

4.2.3. Codes intercomparison

From Fig. 8 (evolution of the aerosol concentration in AB1 test) none of the calculations reproduce the observed quasi-steady state before the sodium pool fire ending, being CPA*_CIEMAT and FEUMIX_IRSN calculations the ones with a better agreement with experiments from about 1000 s after the start of the fire onwards. MELCOR code shows a good quantitative prediction of the maximum airborne concentration.

Regarding AMMD in AB1 test (Fig. 9) for the AB1 test, CIEMAT's calculation shows the best fit to the experimental decrease rate (lower decrease rates can be observed in the rest of calculations). Considerable smaller particles sizes are predicted by CPA_ENEA, FEUMIX_IRSN and MELCOR_ENEA calculations.

Fig. 10 shows the final sodium mass distribution as a fraction of the total depleted mass of sodium. As noted above, sedimentation is the governing deposition mechanism. In addition, the total mass of deposited sodium is presented as an embedded table in the figure. CPA*_CIEMAT and FEUMIX_IRSN show a good consistency with test "data", however CPA*_GRS calculation shows substantial deviations both in total depleted mass and in its distribution. Even though CPA and CONTAIN aerosol models are based both in MAEROS code (Gelbard, 1982), CONTAIN_GRS shows a remarkable good fit to data regarding Na mass distribution. The discrepancies observed between CIEMAT and GRS calculations point out the relevance of the f_i factors setting in CPA* code. In general, it seems that all the codes might overestimate the importance of thermophoresis as a deposition mechanism, predicting a higher fraction of deposition on the walls and vertical surfaces compared to the horizontal ones. It is worth noting that the subestimation of the settling is probably higher considering the approach used: the burn pan modeled as a deposition surface during all the calculation. During the sodium pool fire, no deposition of aerosols is expected onto this surface due to the high level of turbulence and the buoyant circulation foreseen. This could be coupled with possible aerosol particle shape experimental deviations from spherical, influencing particle-particle interaction and dynamics.

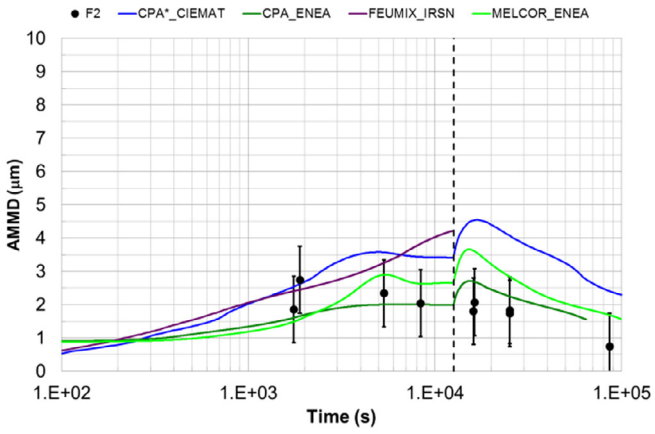

Fig. 15. AMMD (F2).

More investigations are in progress in order to characterize the aerosol behavior and the quantitative discrepancies with the experimental data. It should be underlined, however, that MELCOR (aerosol source is modeled with and imposed mass input) and CONTAIN show a reasonable prediction for the mass fractions deposited.

In AB2 (Figs. 11–13), GRS and IRSN calculations overpredict concentration during the fire, whereas CIEMAT calculations fit data quite consistently. Contrarily, though, the best AMMD fit to data are those of CIEMAT and GRS, whereas ENEA and IRSN notably underestimate. As for the final mass distribution, what said above for AB1 is entirely applicable.

The evolution of the airborne concentration in F2 is presented in Fig. 14. Even though no full credit can be given to the trend showed by measurements due to the uncertainties associated and the non-well mixed atmosphere, CPA*_CIEMAT and CPA_ENEA seems to be close to data maximum (FEUMIX and MELCOR being farther). However, given how data were taken, it is highly likely that measured concentration cannot be compared with an average concentration in the vessel.

4.3. Particles ageing assessment

A simplified version of the ageing model developed by Mathe et al. (2015) has been implemented in CPA* to estimate the chemical evolution of the aerosols produced by a sodium fire during their interaction with steam and CO_2 in the atmosphere. Thus, this section only shows results from CPA* for the tests AB1 and AB2 in which particle composition was measured.

4.3.1. Data analysis

In AB1 and AB2 tests oxygen concentration was measured continuously by two identical monitors that sampled atmosphere from high and low elevations (+6.0 m and -6.7 m, respectively). The composition of containment atmosphere in mole percent is available in tabular form in Hilliard et al. (1979) for AB1 and AB2 tests. Measurements show that atmosphere composition was rather similar at the two locations (for each time data are given for only one location, though).

Samples of suspended aerosol were taken on fluorocarbon membrane filters at different times and protected from laboratory air until analyzed for chemical composition. Aerosol samplers are located at 10 locations from high, low and mid regions in the vessel and at different radial and circumferential positions. Aerosol chemical analysis at different times is available in tabular form in Hilliard et al. (1979) for AB1 test. Besides, samples of deposited aerosol mass on horizontal surfaces were taken from several locations. Data are available in tabular form in Hilliard et al. (1979) for AB1 and AB2 tests. Therefore, no withdrawal uncertainty is associated to gas and particle compositions.

4.3.2. Ageing model predictions

Experimental O_2 mole percent in the vessel atmosphere is shown in Figs. 16 and 17 (AB1 and AB2, respectively). Both tests show a moderate reduction of O_2 concentration during the burning time, from 19.8% (600 s) down to 15.7% in AB1 and from 20% to 16.9% in AB2. In both CPA* simulations this trend is captured and the accuracy shown is reasonable. As for aerosol speciation, experimental data is only available for AB1 test as mass fraction of the involved species at discrete times (16, 46, 190, 610 and 7200 min); calculations extended up to 160 min though, so a limited number of comparisons are set below.

One of the main observations in AB1 was that no Na_2O was found out of the burn pan (Fig. 18). Two explanations might be postulated: Na_2O is formed on the pool surface and it never leaves the pan, which is contrary to the temperature threshold observed

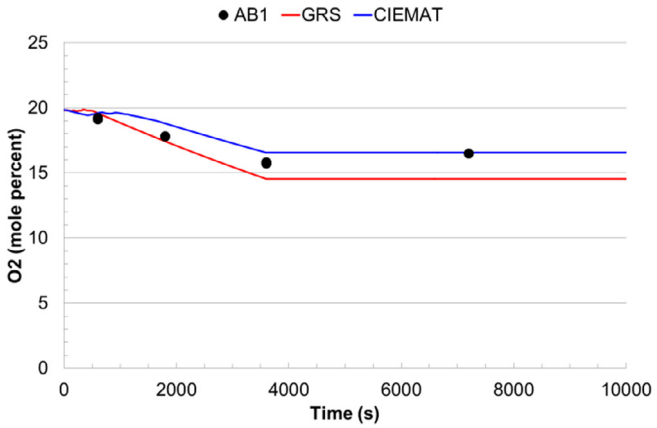

Fig. 16. O_2 mole percent in atmosphere (AB1).

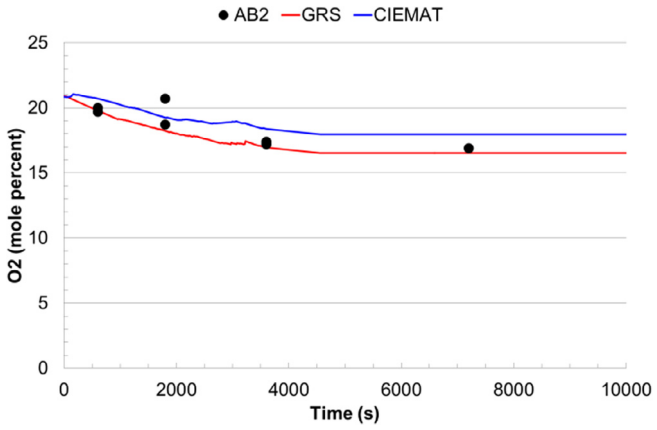

Fig. 17. O_2 mole percent in atmosphere (AB2).

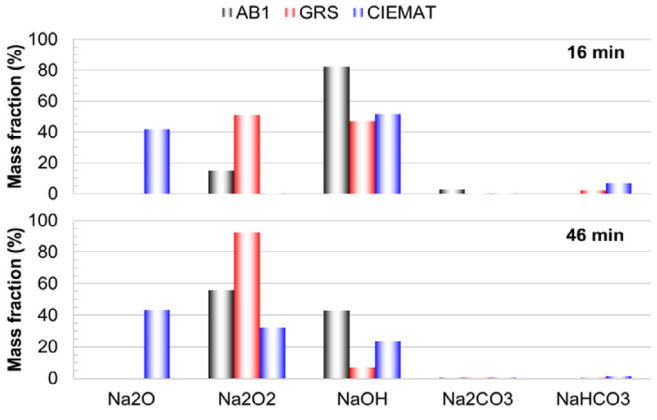

Fig. 18. Suspended species (AB1).

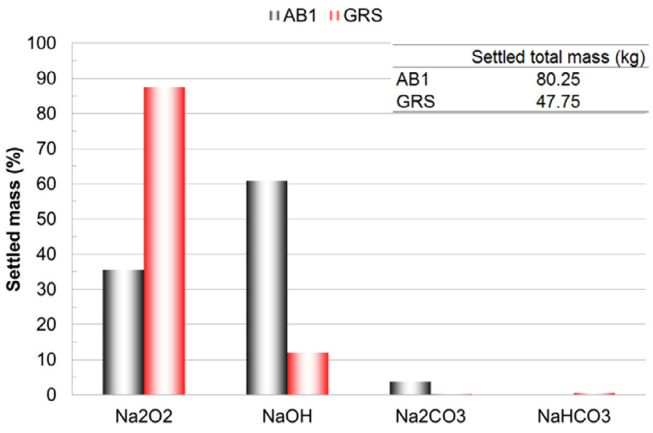

Fig. 19. Settled mass percent of species (AB1).

by Newman for Na surface oxidation (T < 800 K) (Newman, 1983); or Na_2O particles are formed in the gas phase but their properties (mainly size and density) are much larger than those of Na_2O_2 particles, so that they settle down quickly and get never exposed to steam.

As for specific observations at given times, at 16 min the aerosol was predominantly NaOH (82%) coming from the reaction of sodium-oxides aerosol particles with the ambient humidity in the atmosphere; the rest distributes mainly between Na_2O_2 (15%) and Na_2CO_3 (3%). Somewhat later (46 min), most airborne aerosols consisted of Na_2O_2 (56%) and NaOH (43%), which indicates the total depletion of the water vapor content in the atmosphere while aerosol formation is still ongoing. From 46 min on the experimental observations look controversial as they indicate the availability of some steam of an unknown source; anyway, those later times are out of the period in which predictions-data comparisons can be set. NaH data are not included in the figure as its share was lower than 1%.

As for CPA* predictions, none of them showed remarkable similarities to data at the two times (16 min and 46 min) at which comparisons are feasible. According to those comparisons, as long as steam is available the ageing model produces less NaOH than observed; in other words, given that the reactions above are diffusion controlled, this means that steam diffusion coefficient is noticeably underestimated. Differences between CIEMAT and GRS indicate that f_3 and f_4 values assumed by GRS fit what experimentally observed (no Na_2O measured airborne), whereas CIEMAT's calculations resulted in a fraction of particles in oxide form. Additionally, discrepancies in the initial atmosphere humidity in both simulations (GRS, 1.9%; CIEMAT, 2.3%), might slightly affect the composition share. As carbonaceous species were hardly formed, no conclusion can be derived as for the model performance in the entire speciation range (i.e., from oxides to bi-carbonates) .

As for the settled aerosols (Fig. 19), data show that particles consist mostly of NaOH (61%) and a good fraction of Na_2O_2 (36%) and a minor share of Na_2CO_3 (3%). As pinpointed above, the ageing model substantially underestimate the transformation to NaOH and to Na_2CO_3 (although this is less noticeable due to little formation, even experimentally). Then, these evidences also indicate a too low diffusion coefficient in the model. In addition to pure chemical considerations, it is noticeable that GRS calculations underestimate sedimentation in about a factor 1.7.

Unfortunately, no data on airborne aerosol composition are available for AB2. Nevertheless, huge discrepancies have been found in settled particles composition: whereas measurements indicated more than 80% of particles in the form of carbonates (Na_2CO_3), GRS estimated that particles would mostly consist of NaOH (greater than95%). Besides, the GRS estimate of settled mass was more than 3 times lower than data.

5. Conclusions

In previous sections the main insights gained into predictability of particles generation and behavior during in-containment pool fires in postulated severe accidents in Na-cooled fast reactors have been described. To do so experimental data from the open literature has been gathered and reviewed to find out suitable data against which to compare predictions coming from a number of

codes, although the main emphasis is done on the ASTEC-Na module for containment analysis (CPA*). This analytical tool has been adapted from LWR to Na-cooled reactors within the frame of the EU-JASMIN project.

Some conclusions can be drawn from all the tasks carried out before and during the analytical exercise:

- The open literature containing experimental data on postulated in-containment source term behavior of SFRs is scarce. Besides, tests characterization are neither as thorough as desirable nor as accurate as necessary for validation purposes.
- The single node approximation seems to be acceptable to simulate the ABCOVE tests, where intense natural circulation was effective in making the gas phase uniform. However, fast experimental transients, where atmosphere becomes temporarily non-uniform might lead to some data-predictions discrepancies.
- The evolution of FAUNA-F2 test was strongly affected by a non-well mixed atmosphere that prevents from any exhaustive comparison between data and single-cell approach estimates to be set, although some qualitative discussion can still be done.
- Some key phenomena for in-containment source term behavior are described by heavily parametrized models in CPA* (i.e., chemical reaction energy released into the vessel atmosphere or particle injection in the gas phase). A sound proposal of default values is not feasible on the current database.
- Broadly speaking, current CPA* modeling allows predicting consistent thermal and aerosol behavior trends, whenever model parameters are adequately set. Specific strong/weak points with respect to other codes cannot be stated due to the database uncertainties and the high parametrization of the Na-specific embedded models.
- The large experimental uncertainties existing in aerosol concentration during the Na-pool fire period, prevent from withdrawing any specific insights regarding models of particle generation and/or aerosol mechanisms in codes, particularly in CPA*. Contrarily, the depletion phase is reasonably captured by CPA*.
- The limited number of comparisons set regarding the ageing model seems to indicate that chemical transformation of oxides to hydroxides is too slow. Nonetheless, a broader validation would be desirable before reaching any firm conclusion.

Beyond any doubt the main takeaway of this first analytical exercise is to support the need of further research along two axis: to feed CPA* with more and better Na-specific models and to build a robust and extensive database that can be used both to support individual models development and to validate more "integral" tools, like CPA*.

Acknowledgments

The authors wish to thank the funding received from the 7th Framework Programme of the European Commission via the JASMIN project (contract number 295803).

References

Beiriger, P., Hopenfeld, J., Silberberg, M., Johnson, R.P., Baurmash, L., Koontz, R.L., 1973. Sofire II User Report (No. AI-AEC–13055). Atomics International, Canoga Park, Calif. (USA).

Brunett, A., Denning, R., Umbel, M., Wutzler, W., 2014. Severe accident source terms for a sodium-cooled fast reactor. Ann. Nucl. Energy 64, 220–229. http://dx.doi.org/10.1016/j.anucene.2013.10.007.

Cherdron, W., Bunz, H., Jordan, S., 1985. Properties of sodium fire aerosols and recalculation of their behaviour in closed containments. Presented at the CSNI Specialist Meeting on Nuclear Aerosols in Reactor Safety, CSNI-95, Karlsruhe, pp. 395–405.

Cherdron, W., Charpenel, J., 1985. Thermodynamic consequences of sodium spray fires in closed containments. Pt. 2 (No. KFK–3831). Kernforschungszentrum Karlsruhe G.m.b.H. (Germany).

Cherdron, W., Jordan, S., 1983. Die Natrium-Brandversuche in der FAUNA-Anlage auf Brandflächen bis 12m2 (No. KfK 3041).

Cherdron, W., Jordan, S., 1980. Determination of sodium fire aerosol process coefficients from FAUNA-experiments, in: NUREG/CR-1724. Presented at the CSNI Specialist Meeting on Nuclear Aerosols in Reactor Safety, CSNI-45, Gatlingburg, Tennessee (USA), pp. 129–138.

Cherdron, W., Jordan, S., Lindner, W., 1990. Die Natriumbrand-Untersuchungen in der FAUNA: Poolbrände und Aerosolverhalten. Kernforschungszentrum Karlsruhe.

Dunbar, I.H., 1985. Aerosol behaviour codes, development, intercomparison and application. Presented at the CSNI Specialist Meeting on Nuclear Aerosols in Reactor Safety, CSNI-95, Karlsruhe, pp. 471–485.

Dunbar, I.H., Fermandjian, J., Bunz, H., L'Homme, A., Lhiaubet, G., Himeno, Y., Kirby, C.R., Mitsutsuka, N., 1984. Comparison of sodium aerosol codes (CEC report No. EUR–9172). Commission of the European Communities.

Fermandjian, J., 1985. Aerosol behaviour codes, development, intercomparison and application. Presented at the CSNI Specialist Meeting on Nuclear Aerosols in Reactor Safety, CSNI-95, Karlsruhe, pp. 486–497.

Gauntt, R.O., Cash, J.E., Cole, R.K., Erickson, C.M., Humphries, L.L., Rodriguez, S.B., Young, M.F., 2005. MELCOR Computer Code Manuals (No. NUREG/CR-6119, SAND 2005–5713).

Gelbard, F., 1982. MAEROS user manual. [LMFBR] (No. NUREG/CR-1391 SAND80-0822).

Girault, N., Cloarec, L., Herranz, L.E., Bandini, G., Perez-Martin, S., Ammirabile, L., 2015. On-going activities in the European JASMIN project for the development and validation of ASTEC-Na SFR safety simulation code, in: ICAPP2015. Presented at the International Congress on Advances in Nuclear Power Plants (ICAPP 2015), Nice (France), pp. 482–494.

Herranz, L.E., Garcia, M., Kissane, M.P., 2012. In-containment source term in accident conditions in sodium-cooled fast reactors: Data needs and model capabilities. Prog. Nucl. Energy 54, 138–149. http://dx.doi.org/10.1016/j.pnucene.2011.07.003.

Herranz, L.E., Garcia, M., Morandi, S., 2013a. Benchmarking LWR codes capability to model radionuclide deposition within SFR containments: An analysis of the Na ABCOVE tests. Nucl. Eng. Des. 265, 772–784. http://dx.doi.org/10.1016/j.nucengdes.2013.05.030.

Herranz, L.E., Kissane, M.P., Garcia, M., 2013b. Comparison of LWR and SFR in-containment source term: Similarities and differences. Prog. Nucl. Energy 66, 52–60. http://dx.doi.org/10.1016/j.pnucene.2013.03.002.

Hilliard, R.K., McCormack, D., Postma, A.K., 1979. Aerosol behavior during sodium pool fires in a large vessel - CSTF tests AB1 and AB2 (No. HEDL-TME 79–28). Hanford Engineering Development Lab.

Hilliard, R.K., McCormack, J.D., Hassberger, J.A., Muhlestein, L.D., 1977. Preliminary results of CSTF aerosol behavior test, AB1. [LMFBR] (No. HEDL-SA-1381).

IAEA, 2012. Status of Fast Reactor Research and Technology Development, IAEA-TECDOC-1691. Vienna.

Jacq, F., Lefévre, B., 1995. FEUMIX 3.4. Manuel théorique (IRSN internal report).

Klein-Hessling, W., Schwinges, b., 1998. CPA Module: Program Reference Manual, Report ASTEC-V0/DOC/01-34.

Langhans, J., 1991. Natrium - Lachenbrand-Vergleichsrech-nungen mit CONTAIN zu den KFK-Versuchen FAUNA 5 und 6 (No. GRS-A-1856). GRS Cologne.

Mathe, E., Kissane, M.P., Petitprez, D., 2015. Improved Modelling of Sodium-Spray Fires and Sodium-Combustion Aerosol Chemical Evolution, in: ICAPP2015. Presented at the International Congress on Advances in Nuclear Power Plants (ICAPP 2015), Nice (France), pp. 601–610.

McCormack, J.D., Hilliard, R.K., Postma, A.K., 1978. Recent Aerosol Tests in the Containment Systems Test Facility (No. HEDL-SA-1686). Hanford Engineering Development Lab., Richland, WA (USA).

Murata, K.K., Williams, D.C., Griffith, R.O., Gido, R.G., Tadios, E.L., Davis, F.J., Martinez, G.M., Washington, K.E., Tills, J., 1997. Code Manual for Contain 2.0: A Computer Code for Nuclear Reactor Containment Analysis (No. NUREG/CR–6533; SAND–97-1735). Nuclear Regulatory Commission, Washington, DC (United States). Div. of Systems Technology; Sandia National Labs., Albuquerque, NM (United States); Tills (Jack) and Associates Inc, Albuquerque, NM (United States).

Newman, R.N., 1983. The ignition and burning behaviour of sodium metal in air. Prog. Nucl. Energy 12, 119–147. http://dx.doi.org/10.1016/0149-1970(83)90020-3.

Scholtyssek, W., Murata, K.K., 1993. Sodium spray and jet fire model development within the CONTAIN-LMR code (SAND–93-2200C). USA.

Souto, F.J., Haskin, F.E., Kmetyk, L.N., 1994. Melcor 1.8.2 Assessment: Aerosol Experiments Abcove Ab5, Ab6, Ab7, and Lace La2 (No. SAND–94-2166). Sandia National Labs., Albuquerque, NM (United States).

Spengler, C., Reinke, N.O., 2016. Adaptation and Assessment of In-Containment Source Term Oriented Models for Sodium Fast Reactors (SFR) within the ASTEC-Na Code, in: ICAPP2016. Presented at the International Congress on Advances in Nuclear Power Plants (ICAPP 2016), San Francisco, CA, pp. 1482–1491.